Rapid Communications

Far- and midinfrared excitation of large amplitude spin precession in the ferromagnetic semiconductor InMnAs

A. Gatilova,[1] E. A. Mashkovich,[1] K. A. Grishunin,[1,2] A. Pogrebna,[1] R. V. Mikhaylovskiy,[1,3] Th. Rasing,[1] P. M. Christianen,[4] N. Nishizawa,[5] H. Munekata,[5] and A. V. Kimel[1,*]

[1]*Institute for Molecules and Materials, Radboud University, Nijmegen 6525 AJ, The Netherlands*
[2]*MIREA–Russian Technological University, Moscow 119454, Russia*
[3]*Department of Physics, Lancaster University, Lancaster LA1 1YB, United Kingdom*
[4]*High Field Magnet Laboratory (HFML-EMFL), Radboud University, Toernooiveld 7, 6525 ED Nijmegen, The Netherlands*
[5]*Laboratory for Future Interdisciplinary Research of Science and Technology, Tokyo Institute of Technology, Yakohama, Kanagava 226-8503, Japan*

(Received 5 June 2019; revised manuscript received 25 November 2019; published 28 January 2020)

Ultrafast laser excitation of the ferromagnetic semiconductor InMnAs is shown to trigger spin precession with the largest amplitude reported for magnetic semiconductors so far. To reveal the electronic transitions mediating the coupling between light and spins, we compared the spin dynamics triggered by short terahertz (photon energy 5 meV) and midinfrared (photon energy 500 meV) pulses. The experiments reveal that terahertz pump pulses excite qualitatively similar spin dynamics, but are 100 times more energy efficient than the mid-IR pulses. This finding shows that in a semiconductor with hole-mediated ferromagnetism intraband electronic transitions mediate ultrafast and the most efficient coupling between light and spins.

DOI: 10.1103/PhysRevB.101.020413

Controlling the magnetic state of media with the lowest possible cost of energy and simultaneously at the fastest possible timescale is a new and great challenge in fundamental magnetism. At the same time this is becoming an increasingly urgent issue in technology, where data centers already consume about 5% of the world electricity production [1]. A femtosecond laser pulse is one of the shortest stimuli in condensed matter physics. Aiming to understand the dynamics of spins triggered by such a stimulus has launched a new field of ultrafast magnetism [2] and has led to a plethora of fundamentally intriguing experimental observations such as ultrafast all-optical magnetization reversal [3] and highly efficient terahertz (THz) emission in metallic magnets [4]. Even after almost 20 years of intense research, the majority of experiments on ultrafast laser-induced magnetization dynamics are still described in terms of a three-temperature model [5]. The model ignores the electronic structure of magnets and suggests that the result of laser excitation is insensitive to the photon energy and only depends on the duration of the laser pulse and the total energy transferred from light to magnet. However, recent demonstrations of magnetic spin response by optical pumping of d-d electronic transitions in iron garnet [6,7], charge transfer in Sr_2IrO_4 [8], as well as f-f transitions in $DyFeO_3$ [9] and $TmFeO_3$ [10] have naturally raised questions about electronic excitations mediating the control of magnetism by light.

Magnetic semiconductors have long been considered as promising materials for optical control of magnetism [11–13]. The discovery of ferromagnetism in III-V (In,Mn)As and (Ga,Mn)As diluted magnetic semiconductors with hole-mediated ferromagnetic exchange interaction [14] initiated a new boom in the area. High susceptibility of semiconductors to optical excitation, stimulated intense discussions about opportunities to control their magnetic properties via a laser-driven modulation of the hole concentration [15,16], i.e., pumping of electronic interband transitions. It was also proposed that a laser-induced increase of the kinetic energy of holes in the valence band, which can be triggered by pumping of intraband electronic transitions, is a major mechanism responsible for a transfer of angular momentum from localized spins to the charge carriers [17–19]. However, the efficiencies of inter- and intraband transitions in optical control of magnetism in magnetic III-V semiconductors have never been compared experimentally.

In order to address the roles of inter- and intraband transitions in the optical control of spins in a magnetic semiconductor with hole-mediated exchange interaction, we performed time-resolved magneto-optical Kerr effect (TR-MOKE) studies of the magnetization dynamics in InMnAs excited by light with two substantially different photon energies: 500 and 5 meV. In particular, we studied a 29-nm thin film of p-doped $In_{1-x}Mn_xAs$ grown on a GaSb/GaAs substrate by low-temperature beam epitaxy [20] with a Mn concentration $x = 0.12$. The hole concentration $p = 1.5 \times 10^{20}$ cm^{-3}, as estimated from low-field Hall measurements. According to static magneto-optic characterization and superconducting quantum interference device measurements, the film is in a ferromagnetic state at low temperatures with its magnetization oriented perpendicular to the sample surface. The sample undergoes a second-order phase transition from a ferro- to paramagnetic state at the Curie temperature $T_C = 65$ K. The

*a.kimel@science.ru.nl

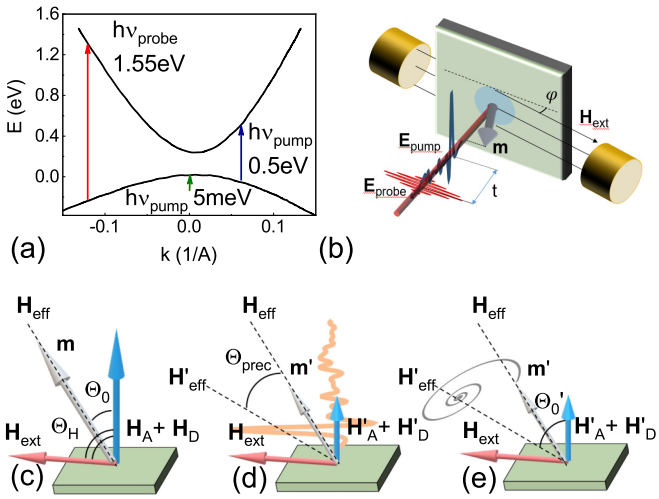

FIG. 1. (a) Schematic representation of the InMnAs band structure (adapted from [26]). Transitions excited by the 1.55 eV probe pulse, and the 5 or 500 meV pump pulses are shown with red, green, and blue arrows, respectively; (b) schematic representation of the TR-MOKE experiment; (c) in equilibrium the magnetization is aligned along $\mathbf{H}_{\text{eff}}$; (d) reorientation of the effective field after excitation is caused by the reduction in the demagnetization and anisotropy; (e) magnetization precession around the new effective field position and magnetization relaxation with time τ_{relax}.

band-gap energy of InMnAs is about 333 meV, which is smaller than the band gap of the materials forming the substrate GaSb/GaAs, 0.72 and 1.44 eV (at 300 K), respectively. The schematic band diagram of InMnAs and the experimentally excited electronic transitions are shown in Fig. 1(a). To excite interband transitions we applied midinfrared (mid-IR) pump pulses with a central photon energy $h\nu_{\text{pump}}^{\text{mid-IR}} = 500$ meV. The pulse duration was 200 fs. To excite intraband electronic transitions, nearly single-cycle THz (far-infrared) pump pulses with a duration 1 ps and the central photon energy $h\nu_{\text{pump}}^{\text{THz}} = 5$ meV were used. The probe pulse had a duration of 100 fs and a central energy of the photons $h\nu_{\text{probe}} = 1.55$ eV. For the measurements we employed an amplified Ti:sapphire laser with a repetition rate of 1 kHz. Generation of the mid-IR and THz pump pulses was achieved through nonlinear optical processes in an optical parametric amplifier (OPA) and in a $LiNbO_3$ crystal [21,22], respectively. The fluence of the mid-IR pump pulses was varied with neutral density filters, while the fluence of the THz pump was adjusted using two wire-grid polarizers. The sample was in a continuous-flow cryostat with optical access via Suprasil B windows which transmit about 64% and 80% of the THz and mid-IR radiation power, respectively. The polarization rotation of the probe beam was measured with the help of a two-diode balanced detection scheme.

The geometry of the MOKE experiments is shown in Fig. 1(b). The polarization rotation of the probe pulse, delayed by the time delay t with respect to the pump pulse, is measured in reflection geometry. Pump and probe pulses are normally incident. Thus, the probe pulse is sensitive to the out-of-plane magnetization component. An applied external magnetic field $\mathbf{H}_{\text{ext}}$ under an angle $\phi_{\text{mid-IR}} = 11^\circ$ and $\phi_{\text{THz}} = 9^\circ$ from the surface plane (near hard-axis direction) is tilting the magnetization towards the surface. The equilibrium position of the magnetization is defined by the effective magnetic field $\mathbf{H}_{\text{eff}}$ given by the vector sum of the anisotropy $\mathbf{H}_{\text{A}}$, demagnetizing $\mathbf{H}_{\text{D}}$ and external magnetic $\mathbf{H}_{\text{ext}}$ fields [(see Fig. 1(c)]. Laser excitation of InMnAs is expected to induce not only longitudinal spin dynamics, e.g., ultrafast demagnetization [18], but also to launch spin precession by changing the direction of $\mathbf{H}_{\text{eff}}$ via ultrafast reduction of the $\mathbf{H}_{\text{A}}$ and $\mathbf{H}_{\text{D}}$ [23] [see Fig. 1(d)]. A reorientation of $\mathbf{H}_{\text{eff}}$ leads to a subsequent transverse spin dynamics, i.e., oscillations of the spins around a nonequilibrium effective magnetic field $\mathbf{H}'_{\text{eff}}$ induced by the excitation.

Excitation of InMnAs with the help of femtosecond laser pulse changes the net magnetization of the medium leading to (i) partial reduction of the magnetization of the material on a timescale of 1 ps [18] and (ii) further demagnetization of the medium on a timescale of 100 ps. Moreover, the laser excitation can also affect magnetic anisotropy either (i) directly due to ionization of magnetic ions [7,24] or (ii) indirectly owing to the dependency of effective anisotropy fields on the magnetization. According to the Callen-Callen law, $K_1 \sim M^2$, where K_1 stays for an out-of plane anisotropy [25]. Afterwards the net magnetization recovers on a timescale of 1 ns. Therefore, even if one assumes that there is no direct effect of light on $\mathbf{H}_{\text{A}}$, from the Callen-Callen power law it is clear that laser excitation can result in a large amplitude spin precession and switching. Although revealing dynamics of $\mathbf{H}_{\text{D}}$ and $\mathbf{H}_{\text{A}}$ can be a difficult task, the experimental procedure of stroboscopic measurements employed here is sensitive only to those changes of $\mathbf{H}'_{\text{eff}}$ that recover in the period between two pump pulses, 2 ms.

Dynamics of the magneto-optical Kerr effect for different values of the applied external magnetic field triggered at 55 K by the mid-IR and THz pump pulses are shown in Figs. 2(a) and 2(b), respectively. All curves are normalized with respect to the magneto-optical signal at equilibrium θ_{K}. Remarkably, the dynamics triggered by mid-IR and THz pump pulses are very similar: ultrafast demagnetization is followed by a relaxation and oscillations of the magneto-optical signal. The demagnetization, i.e., the longitudinal dynamics of the magnetization, occurs at two different timescales: 2 ± 1 ps and 7.5 ± 1.5 ps [see Fig. S1(b) in [27]]. We note that ultrafast demagnetization is a particular case of longitudinal magnetization dynamics. The timescale of this dynamics is defined by the exchange interaction. The strength of this interaction can be expressed in terms of an effective magnetic field $kT_{\text{C}}/h\gamma \approx 1000$ kOe, where $\gamma = 2.8$ GHz/kOe is the gyromagnetic ratio for the spin of a Mn^{2+} ion, k is Boltzmann constant, and h is the Planck constant. Obviously, a magnetic field much lower than 1000 kOe would not be able to affect the longitudinal relaxation. One can see from Figs. 2(a) and 2(b), the dynamics for delays longer than 10 ps can be substantially changed by a modest increase of the applied magnetic field from 1.7 to 3.4 kOe. This fact is a strong indication that, similar to experiments on ferromagnetic metals [28–31], the relaxation and the oscillations are due to transverse magnetization dynamics. The relaxation time τ_{relax} [see Fig. 2 (c)] decreases on the applied magnetic field until it reaches the value of

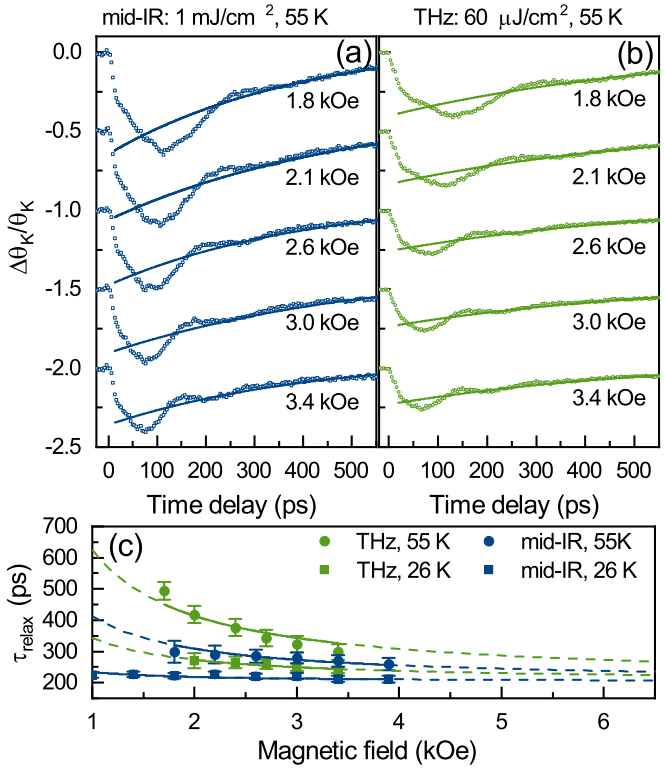

FIG. 2. Time-resolved-MOKE measured at 55 K for different values of the applied magnetic field upon mid-IR (a) and THz (b) excitation. Solid lines show exponential relaxation of the photoinduced dynamics. (c) Relaxation time τ_{relax} of the signal extracted from the raw data after mid-IR and THz excitation at ambient temperatures of 55 and 26 K.

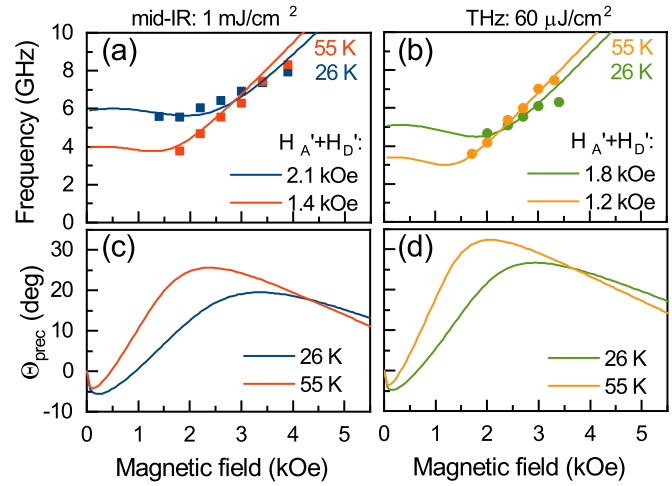

FIG. 3. (a),(b) The dependence of the precession frequency on the external magnetic field measured at 26 and 55 K for 1 mJ/cm^2 mid-IR and 60 μJ/cm^2 THz excitation, respectively. Solid lines represent the estimated lines of ferromagnetic resonance (FMR) with given values of $|\mathbf{H}'_{\text{A}} + \mathbf{H}'_{\text{D}}|$. (c),(d) The precession angle calculated for the aforementioned FMR lines as a function of the external magnetic field shown for mid-IR and THz excitation, respectively.

215 ± 8 ps and gets stabilized there: $\tau_{\text{relax}} = 215 + A/\text{H}_{\text{ext}}$. This time $\tau = 215 \pm 8$ ps, which is independent of the applied magnetic field and ambient temperature, can be assigned to the recovery of the magnetization due to recombination of electrons from the excited states and cooling of the sample [see also Fig. S1(a) in [27]].

To deduce the oscillatory part of the dynamics, we subtracted the exponential decay with the characteristic time τ_{relax} from the raw data. Regarding very large damping it is safe to assume that on a timescale of the damped oscillations the direction of $\mathbf{H}'_{\text{eff}}$ does not change. The obtained oscillations were analyzed by Fast Fourier transformation (FFT). The phenomenological (Gilbert) damping parameter was found to be $\alpha = 1/(t_{\text{damp}} f) = 0.5$ at high fields, where t_{damp} and f are the damping time and frequency of the subtracted oscillations.

The obtained central frequency of the oscillations as a function of the applied magnetic field for two distinct temperatures is shown with dots in Figs. 3(a) and 3(b) for mid-IR and THz excitation, respectively. For both photon energies the two distinct regimes of spin precession are seen at the temperature far below and in the vicinity of T_{C}. Note that the frequency of the experimentally observed heavily damped oscillations appears to be in a good agreement with the estimates (solid lines) obtained from the analytical solution of the Landau-Lifshitz-Gilbert equation with the help of the Smith-Suhl formula [32] [see Eq. (S1) in [27]]. In the estimates, the sum of the residual anisotropy and demagnetizing fields $|\mathbf{H}'_{\text{A}} + \mathbf{H}'_{\text{D}}|$ is a parameter that determines the oscillations frequency and the new effective field position at an angle Θ'_0 [see Eq. (S2) in [27]]. Comparing $|\mathbf{H}'_{\text{A}} + \mathbf{H}'_{\text{D}}|$ in Figs. 3(a) and 3(b) shows that 20 times weaker THz excitation leads to a higher reduction of anisotropy and demagnetizing fields.

The precession angle Θ_{prec} is calculated as a difference between initial and new effective field position at angles Θ_0 and Θ'_0, respectively:

$$\Theta_{\text{prec}} = \Theta_0 - \Theta'_0, \tag{1}$$

where the Θ_0 value is extracted from polar Kerr measurements [see Eq. (S3) in [27]]. The dependence of the calculated Θ_{prec} on an external magnetic field is shown in Figs. 3(c) and 3(d) for mid-IR and THz excitation, respectively. It is seen that larger precession angles are achieved in the case of smaller values of residual $|\mathbf{H}'_{\text{A}} + \mathbf{H}'_{\text{D}}|$. The large precession angle $\Theta_{\text{prec}} = 32^\circ$ is determined for $H_{\text{ext}} = 2.0$ kOe at 55 K after THz excitation.

Figure 4(a) shows the photoinduced change of the polarization rotation $\Delta\theta_{\text{K}}$ normalized on the MOKE angle at equilibrium θ_{K} for mid-IR and THz excitation, respectively. It is seen that for the same experimental conditions (at 26 K and 3.3 kOe), a mid-IR pulse with fluence 7 mJ/cm^2 triggers the same spin dynamics as a THz pulse with a 100 times lower fluence: 0.065 mJ/cm^2. Note that in the InMnAs film the absorbed THz radiation is expected to be smaller than that of mid-IR light due to the much longer wavelength of the THz.

The observed time traces show no dependence on polarization of the pump pulses for both photon energies, which suggests a heat-induced nature of the observed dynamics. To understand the excitation mechanism for both photon energies, we show in Fig. 4(b) the maximum value of $\Delta\theta_{\text{K}}/\theta_{\text{K}}$ as a function of intensity of the mid-IR and THz pulses, recalculated to the amount of photons N per magnetic site (ph/Mn). Although the dependencies of $\max(\Delta\theta_K/\theta_K)$ on the

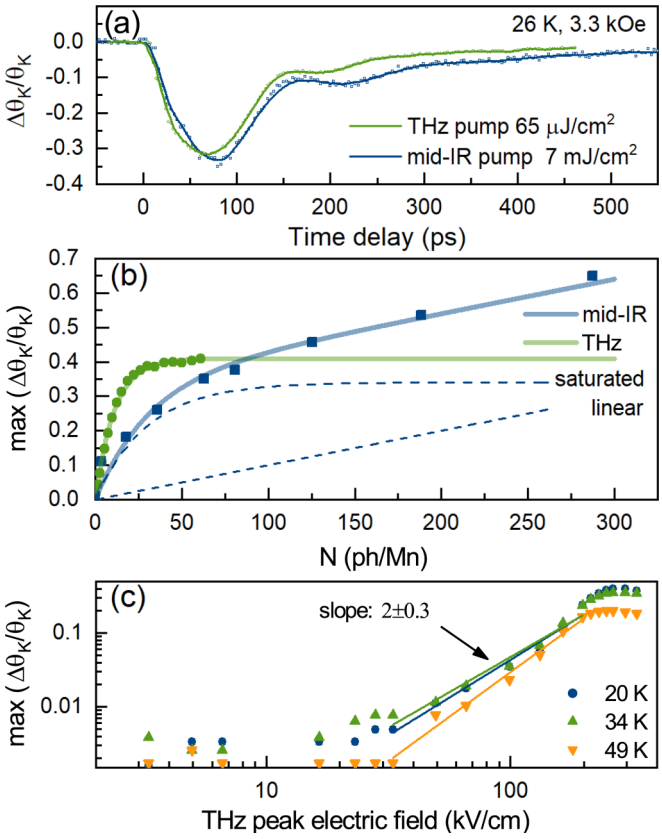

FIG. 4. (a) Relative change of the polarization rotation for mid-IR and THz pump pulses with fluences of 7 mJ/cm^2 and 65 μJ/cm^2, respectively. (b) The maximum photoinduced change in the Kerr rotation upon mid-IR (solid blue curve) and THz (solid green curve) excitation as a function of the number of photons per Mn. The mid-IR dependence consists of the sum of a saturated and a simple linear response (dashed blue curves). (c) The maximum photoinduced change in the Kerr rotation upon THz excitation as a function of peak THz electric field shown for different temperatures. Solid lines represent linear fits with the slope 2 ± 0.3.

number of photons for inter- and intraband excitation seem to be strikingly different, one can also find similarities between them and interpret the data in Fig. 4(b) in a following way. If one fits the IR dependence above $N = 100$ to linear and then extrapolates the line to the left, it will intercept the ordinate between 0.3 and 0.4, which is close to the saturation value obtained for the curve corresponding to the THz pump. It means that the dependence obtained for mid-infrared pump can be represented as a sum of a linear increase and a curve similar to that obtained for the THz pump, with close values of saturation level and saturating fluence. The linear part can be attributed to the heating, which is 100 times smaller for the THz excitation and thus not visible in the experiment. The part of the dependence which shows the saturation can have the same origin in both cases. However, despite the suggested hypotheses, we admit that revealing the origin of the fluence dependence and how it changes with photon energy remains a subject for future studies.

Alternatively, one can also interpret the data emphasizing the differences between the outcomes of the mid-infrared and THz experiment. We note that the mechanism of subpicosecond demagnetization of InMnAs induced by femtosecond laser pulses in the midinfrared spectral range was studied experimentally and theoretically in Ref. [18]. It was suggested that the mechanism relies on photogeneration of hot holes, the manifestation of which is represented by the linear growth of $\max(\Delta\theta_K/\theta_K)$ upon an increase of the mid-IR pump fluence. According to Callen-Callen power law [25], $K_1 \sim M^2$, ultrafast demagnetization also results in a reduction of $\mathbf{H}_A$, and subsequent reorientation of $\mathbf{H}_{\text{eff}}$. However, it is not the primary mechanism that triggers the transverse spin dynamics. For a very similar magnetic semiconductor GaMnAs [24], it was argued that ionizationlike transition on Mn^{2+} ions ($Mn^{2+} \rightarrow Mn^{3+}$) as a result of interband photoexcitation changes the orbital momentum of Mn ions and thus affects the magnetic anisotropy of the compound directly. Saturation of the aforementioned transitions could be seen in a saturated curve of the mid-IR dependence shown in Fig. 4(b).

Photoionization $Mn^{2+} \rightarrow Mn^{3+}$ might be efficiently caused also by THz radiation in InMnAs. In Ref. [33] it was shown that a THz electric field above a threshold value (about 90 kV/cm) is able to generate electron-hole pairs in *p*-doped InAs via impact ionization. The energy required for this photoionization is comparable with the energy of the intraband transition triggered by THz excitation in our experiment. To show this, we plot the measured $\max(\Delta\theta_K/\theta_K)$ as a function of THz peak electric field [see Fig. 4(c)] on a logarithmic scale. On top of the quadratic dependence that is expected in the measurements [$N(\text{ph/Mn}) \sim I_{\text{THz}} \sim E^2_{\text{THz}}$], a threshold behavior with a threshold value of 35 kV/cm is seen for data at all temperatures. Such an electric field is in the ballpark of electric fields that generate electron-hole pairs in InAs and thus they must be able to ionize Mn ions in InMnAs as well. The observed temperature-independent saturation of the magneto-optical signal can also be explained as a peculiarity of impact ionization of the Mn^{2+} ions in InMnAs. Regarding the limited amount of Mn ions in the material, a THz-induced increase of the concentration of the ionized ions decreases the probability of the ionization. However, further studies of InMnAs with different Mn concentrations are necessary to verify this hypothesis.

Interestingly, the electron excitation into conduction band via impact ionization might play a significant role not only in an ultrafast change of magnetic anisotropy, but also in the demagnetization process, since a THz pulse with such a small fluence as 65 μJ/cm^2 is able to induce demagnetization of at least 25% (see Fig. S1(c) in [27]). This statement has to be verified in further experiments on THz-induced magnetization dynamics, since it contradicts the contemporary understanding of ultrafast demagnetization in ferromagnetic (III,Mn)V semiconductors [17].

In summary, we have compared the efficiency of inter- and intraband transitions in optical control of magnetism in magnetic semiconductor InMnAs. In particular, it is found that a THz photon, despite 100 times lower energy, has a larger impact on the magnetization of InMnAs than a photon in the midinfrared spectral range. Similarly to the finding reported recently in Ref. [34], the strength of the effect of light on magnetism is more a function of the photon flux than the total energy deposited into the sample. Therefore,

our finding opens up another avenue in experimental and theoretical studies of ultrafast laser-induced magnetization dynamics.

The authors thank S. Semin, P. Albers, F. Janssen, and Ch. Berkhout for technical support. This research has received funding from the European Union's Horizon 2020 research and innovation program under FET-Open Grant Agreement No. 713481(SPICE), the Russian Foundation for Basic Research (18-02-40027 and 18-52-53030), the European Research Council ERC Grant Agreement No. 339813 (Exchange), de Nederlandse Organisatie voor Wetenschappelijk Onderzoek (NWO), and was supported by HFML-RU/NWO-I, member of the European Magnetic Field Laboratory (EMFL). H.M. acknowledges partial support for the present work from KAKENHI (JSPS) 18H03878.

[1] Nicola Jones, How to stop data centres from gobbling up the world's electricity, Nature (London) **561**, 163 (2018).

[2] E. Beaurepaire, J.-C. Merle, A. Daunois, and J.-Y. Bigot, Ultrafast Spin Dynamics in Ferromagnetic Nickel, Phys. Rev. Lett. **76**, 4250 (1996).

[3] C. D. Stanciu, F. Hansteen, A. V. Kimel, A. Kirilyuk, A. Tsukamoto, A. Itoh, and Th. Rasing, All-Optical Magnetic Recording with Circularly Polarized Light, Phys. Rev. Lett. **99**, 047601 (2007).

[4] T. Seifert, S. Jaiswal, U. Martens, J. Hannegan, L. Braun, P. Maldonado, F. Freimuth, A. Kronenberg, J. Henrizi, I. Radu *et al.*, Efficient metallic spintronic emitters of ultrabroadband terahertz radiation, Nat. Photon. **10**, 483 (2016).

[5] M. B. Agranat, S. I. Ashitkov, A. B. Granovskii, and G. I. Rukman, Interaction of picosecond laser pulses with the electron, spin, and phonon subsystems of nickel, Zh. Eksp. Teor. Fiz **86**, 10 (1984).

[6] A. Stupakiewicz, K. Szerenos, D. Afanasiev, A. Kirilyuk, and A. V. Kimel, Ultrafast nonthermal photo-magnetic recording in a transparent medium, Nature (London) **542**, 71 (2017).

[7] A. Stupakiewicz, K. Szerenos, M. D. Davydova, K. A. Zvezdin, A. K. Zvezdin, A. Kirilyuk, and A. V. Kimel, Selection rules for all-optical magnetic recording in iron garnet, Nat. Commun. **10**, 612 (2019).

[8] D. Afanasiev, A. Gatilova, D. J. Groenendijk, B. A. Ivanov, M. Gibert, S. Gariglio, J. Mentink, J. Li, N. Dasari, M. Eckstein, Th. Rasing, A. D. Caviglia, and A. V. Kimel, Ultrafast Spin Dynamics in Photodoped Spin-Orbit Mott Insulator Sr_2IrO_4, Phys. Rev. X **9**, 021020 (2019).

[9] R. V. Mikhaylovskiy, T. J. Huisman, A. I. Popov, A. K. Zvezdin, Th. Rasing, R. V. Pisarev, and A. V. Kimel, Terahertz magnetization dynamics induced by femtosecond resonant pumping of Dy^{3+} subsystem in the multisublattice antiferromagnet $DyFeO_3$, Phys. Rev. B **92**, 094437 (2015).

[10] S. Baierl, M. Hohenleutner, T. Kampfrath, A. K. Zvezdin, A. V. Kimel, R. Huber, and R. V. Mikhaylovskiy, Nonlinear spin control by terahertz-driven anisotropy fields, Nat. Photon. **10**, 715 (2016).

[11] E. L. Nagaev, Photoinduced magnetism and conduction electrons in magnetic semiconductors, Phys. Status Solidi B **145**, 11 (1988).

[12] G. Güntherodt, P. Wachter, and D. M. Imboden, Energy level scheme and the effect of magnetic order on the optical transitions in europium chalcogenides, Phys. Kondens. Mater. **12**, 292 (1971).

[13] M. M. Afanasiev, M. E. Kompan, and I. A. Merkulov, Increase of Curie-temperature of magnetic semiconductors by illumination, JETP Lett. **231**, 570 (1976).

[14] T. Dietl, H. Ohno, and F. Matsukura, Hole-mediated ferromagnetism in tetrahedrally coordinated semiconductors, Phys. Rev. B **63**, 195205 (2001).

[15] E. Kojima, R. Shimano, Y. Hashimoto, S. Katsumoto, Y. Iye, and M. Kuwata-Gonokami, Observation of the spin-charge thermal isolation of ferromagnetic $Ga_{0.94}Mn_{0.06}As$ by time-resolved magneto-optical measurements, Phys. Rev. B **68**, 193203 (2003).

[16] S. Koshihara, A. Oiwa, M. Hirasawa, S. Katsumoto, Y. Iye, C. Urano, H. Takagi, and H. Munekata, Ferromagnetic Order Induced by Photogenerated Carriers in Magnetic III-V Semiconductor Heterostructures of (In,Mn)As/GaSb, Phys. Rev. Lett. **78**, 4617 (1997).

[17] L. Cywiński and L. J. Sham, Ultrafast demagnetization in the *sp-d* model: A theoretical study, Phys. Rev. B **76**, 045205 (2007).

[18] J. Wang, C. Sun, J. Kono, A. Oiwa, H. Munekata, Ł. Cywiński, and L. J. Sham, Ultrafast Quenching of Ferromagnetism in InMnAs Induced by Intense Laser Irradiation, Phys. Rev. Lett. **95**, 167401 (2005).

[19] J. Wang, Ł. Cywiński, C. Sun, J. Kono, H. Munekata, and L. J. Sham, Femtosecond demagnetization and hot-hole relaxation in ferromagnetic $Ga_{1-x}Mn_xAs$, Phys. Rev. B **77**, 235308 (2008).

[20] T. Schallenberg and H. Munekata, Preparation of ferromagnetic (In,Mn)As with a high Curie temperature of 90 K, Appl. Phys. Lett. **89**, 042507 (2006).

[21] M. I. Bakunov, S. B. Bodrov, and E. A. Mashkovich, Terahertz generation with tilted-front laser pulses: Dynamic theory for low-absorbing crystals, J. Opt. Soc. Am. B **28**, 1724 (2011).

[22] H Hirori, A Doi, F Blanchard, and K Tanaka, Single-cycle terahertz pulses with amplitudes exceeding 1 MV/cm generated by optical rectification in $LiNbO_3$, Appl. Phys. Lett. **98**, 091106 (2011).

[23] R. R. Subkhangulov, H. Munekata, Th. Rasing, and A. V. Kimel, Laser-induced spin dynamics in ferromagnetic (In,Mn)As at magnetic fields up to 7 T, Phys. Rev. B **89**, 060402(R) (2014).

[24] T. Matsuda and H. Munekata, Mechanism of photoexcited precession of magnetization in (Ga,Mn)As on the basis of time-resolved spectroscopy, Phys. Rev. B **93**, 075202 (2016).

[25] E. R. Callen and H. B. Callen, Static magnetoelastic coupling in cubic crystals, Phys. Rev. **129**, 578 (1963).

[26] M. Bhowmick, T. R. Merritt, G. A. Khodaparast, Bruce W. Wessels, Stephen A. McGill, D. Saha, X. Pan, G. D. Sanders, and C. J. Stanton, Time-resolved differential transmission in MOVPE-grown ferromagnetic InMnAs, Phys. Rev. B **85**, 125313 (2012).

[27] See Supplemental material at http://link.aps.org/supplemental/10.1103/PhysRevB.101.020413 for data on THz-induced demagnetization, for the Smith-Suhl formula in strongly anisotropic ferromagnets, and for the estimation of the effective field position at given values of the external field.

[28] M. van Kampen, C. Jozsa, J. T. Kohlhepp, P. LeClair, L. Lagae, W. J. M. de Jonge, and B. Koopmans, All-Optical Probe of Coherent Spin Waves, Phys. Rev. Lett. **88**, 227201 (2002).

[29] M. Vomir, L. H. F. Andrade, L. Guidoni, E. Beaurepaire, and J.-Y. Bigot, Real Space Trajectory of the Ultrafast Magnetization Dynamics in Ferromagnetic Metals, Phys. Rev. Lett. **94**, 237601 (2005).

[30] A. A. Rzhevsky, B. B. Krichevtsov, D. E. Bürgler, and C. M. Schneider, Magnetization dynamics induced by ultrashort optical pulses in Fe/Cr thin films, Phys. Rev. B **75**, 224434 (2007).

[31] M. C. Langner, C. L. S. Kantner, Y. H. Chu, L. M. Martin, P. Yu, J. Seidel, R. Ramesh, and J. Orenstein, Observation of Ferromagnetic Resonance in $SrRuO_3$ by the Time-Resolved Magneto-Optical Kerr Effect, Phys. Rev. Lett. **102**, 177601 (2009).

[32] A. Gurevich and G. Melkov, *Magnetization oscillations and waves* (CRC, Boca Raton, FL, 1996).

[33] I.-Chen Ho and X.-C. Zhang, Driving intervalley scattering and impact ionization in InAs with intense terahertz pulses, Appl. Phys. Lett. **98**, 241908 (2011).

[34] E. A. Mashkovich, K. A. Grishunin, R. V. Mikhaylovskiy, A. K. Zvezdin, R. V. Pisarev, M. B. Strugatsky, P. C. M. Christianen, Th. Rasing, and A. V. Kimel, Terahertz Optomagnetism: Nonlinear THz Excitation of GHz Spin Waves in Antiferromagnetic $FeBO_3$, Phys. Rev. Lett. **123**, 157202 (2019).